# CELLULOSE PHOSPHATE FROM OIL PALM BIOMASS AS POTENTIAL BIOMATERIALS

Wan Rosli Wan Daud,[a,*] Mohamad Haafiz Mohamad Kassim,[a] and Azman Seeni [b]

The present study investigates cellulose phosphate from oil palm biomass (OPEFB-CP) as a potential biomaterial. To this effect, oil palm biomass microcrystalline cellulose (OPEFB-MCC) was phosphorylated using the $H_3PO_4$/ $P_2O_5$/ $Et_3PO_4$/ hexanol method. Characterization of OPEFB-CP was performed using Scanning Electron Microscopy (SEM), Energy Dispersive X-ray (EDX), Fourier Transform Infrared (FTIR) spectroscopy, thermogravimetry (TG), and X-ray diffraction (XRD). The cytotoxicity evaluation of OPEFB-CP was conducted on mouse connective tissue fibroblast cells (L929) using MTS Assay analysis, and the proliferation rate of OPEFB-CP on L929 was assessed by the indirect extraction method, whilst mineralization assessment was carried out by immersion of the material in Simulated Body Fluid (SBF) for 30 days. Disruption of the crystalline structure of OPEFB-MCC, changes in surface morphology of OPEFB-CP, the presence of new FTIR peaks on OPEFB-CP at 2380 $cm^{-1}$ and 1380 $cm^{-1}$, and a smaller rate of mass loss of OPEFB-CP are indications of a successful grafting of phosphate groups. OPEFB-CP showed non-cytotoxic *in vitro* biocompatibility after 72h exposure with an IC-50 value 45mg/mL and a proliferation rate of up to 8 days with no change in cells morphology below the IC-50 concentration. Apatite formation was observed on OPEFB-CP surfaces after 30 days in SBF with a Ca:P ratio of 1.85.

*Keywords: Oil Palm biomass; Cellulose phosphate; Biomaterial; In vitro Biocompatibility; Cytotoxicity; Bioactivity; Simulated Body Fluid (SBF )*

*Contact information a: Bio-Resources, Paper and Coating Division, School of Industrial Technology, Universiti Sains Malaysia, 11800 Pulau Pinang, Malaysia; b: : Advanced Medical and Dental Institute, Universiti Sains Malaysia, 13200 Bertam, Penang, Malaysia; * Corresponding author: wanrosli@usm.my*

## INTRODUCTION

Biomaterial refers to any materials, either natural or man-made that are intended to interface with biological systems or biomedical device for evaluating, treating, augmenting, or replacing any tissue, organ, or function of the body (Nair and Laurencin 2005; 2007). The essential characteristics that must be present to qualify the materials as biomaterials are their biocompatiblity and bioactivity capability (Entcheva et al. 2004).

Biocompatibility is the ability of a material to perform with an appropriate host response in a specific application. From the clinical perspective these materials do not produce toxic or injurious reaction in addition to not causing immunological rejection (Matthew 2002; Vepari et al. 2007; Correlo et al. 2008). Bioactivity, on the other hand, refers to the capability of a material to mineralize in physiological environment and in orthopaedic applications. Bioactivity is often referred to as the ability of a material to

induce the formation of an apatite layer (calcium phosphate layer) in simulated plasma solutions (Granja et al. 2005; Granja and Barbosa. 2001).

Several classes of materials such as ceramics, metals, glasses, and natural and synthetic polymeric materials have been investigated as biomaterials for medical use, especially in tissue engineering and orthopaedic applications (Burg et al. 2000; Nair and Laurencin 2005; Barbosa et al. 2005; Correlo et al. 2008). However, some of these materials have also drawbacks and limitations, such as metallic implants that are used in the repair of bone that cause stress shielding and bone resorption due to the elasticity mismatch with the surrounding bone. Despite its extensive application in bone reconstruction the modulus of elasticity of relatively less rigid titanium is still five times higher than human bone, and it still presents other limitations (Li et al. 1997a; Nair and Laurencin 2005). Ceramic materials may not be favourable as bone repairing material in some applications because of their susceptibility to fatigue failure and low fracture toughness.

Due to the socioeconomic situation of the modern world and environmental concerns, interest in using natural biodegradable polymers, such as cellulose, is on the rise. Their biodegradability, low toxicity, low disposal costs, low manufacturing cost related to large agricultural availability, and renewability make them excellent candidates for biomedical application purposes (Li et al. 1997a; Barbosa et al. 2005; Vepari et al. 2007). Furthermore, their versatility of chemical structures and their well-known chemistry allow the development of advanced functionalized materials that can match several varied requirements. One good example is cellulose phosphate, which is used for the treatment of calcium (Ca) metabolism-related diseases, such as renal stones. This capability is due to its high Ca binding capacity, associated with its lack of toxicity and indigestibility. Cellulose phosphate (CP) has shown potential as a biomaterial for orthopaedic applications, as investigated by several researchers (Barbosa et al. 2005; Nair and Laurencin 2005; Granja et al. 2001). Hence, the rationale to develop and create a new biomaterial for medical applications by using this natural biodegradable polymer is a rational approach (Nair and Laurencin 2005; Barbosa et al. 2005; Alriols et al. 2009).

Cellulose, which is produced by plants as well as by microorganisms, is the world's most abundant natural polymer. It is a linear homopolymer of glucose $(C_6H_{10}O_5)_n$, with n ranging from 500 to 5000. Apart from its insolubility in water and biodegradability, other unique properties such as nontoxicity (monomer residues are not hazardous to health), high swelling ability by simple chemical modification, stability over a wide range of temperature and pH, and a broad variety of chemical structures that can be synthesized, make cellulose the polymer group with the longest and widest medical applications (Kaputskii et al. 2007; Muller et al. 2006; Fricain et al. 2002).

In order to increase its usefulness, cellulose can be chemically modified by substituting the free hydroxyl groups on its backbone with various functional groups to generate new cellulose derivatives that can fulfill the specific needs of various applications. Among the more prominent cellulose derivatives are cellulose acetate and carboxymethylcellulose. However, this renewed interest has seen the emergence of new biopolymers, such as cellulose phosphate, which has been generating recent research attention.

In biomedical applications cellulose derivatives have been extensively investigated as dressings for treating surgical incisions, burns and wounds, as hemodialysis membranes, as coating materials for drugs and drug-releasing scaffolds, and for various dermatological disorders (Entcheva et al. 2004; Nair and Laurencin 2005; Granja et al. 2005). Oxidized cellulose was used as a wound dressing and has been proposed for bone regeneration. Regenerated cellulose hydrogels (cellulose regenerated by the viscose process, CRV) have been investigated as implantable materials in orthopedic surgery, as sealing materials for the femoral component in hip prostheses, in place of the acrylic cement (Granja et al. 2005).

Nevertheless, a full bioactive character cannot be attributed to normally occurring cellulose because of its lack of osteoinduction. Phosphorylation was therefore anticipated as the means to enhance cellulose bioactivity. Once implanted, phosphorylated cellulose could promote the formation of calcium phosphate (which has a closer resemblance to bone functionality), hence ensuring a satisfactory bonding at the interface between hard tissue and biomaterial. The phosphorylated material was found to be non-cytotoxic in cultured human osteoblasts as well as fibroblasts cultures, having the ability to induce the formation of an apatite layer under simulated physiological conditions (Barbosa et al. 2005; Granja et al. 2005).

In Malaysia, over 15 million tons of empty fruit bunches (EFB) from palm oil (*Elaeis guineensis*) waste residues are generated annually from oil palm industries. This lignocellulosic waste, generated after the oil extraction, is a good source of cellulose, lignin, and hemicelluloses that can be used in many process industries. Attempts have been made to utilize these residues, one of which is conversion into cellulose pulp for papermaking (WanRosli et al. 1998; 2007). Although it was considered a value-added product, it is nevertheless a relatively "low end" one, where the price per tonne is rather low. Hence, other utilization alternatives are sought, one of which is conversion into cellulose derivatives, such as carboxymethylcellulose (CMC) and cellulose acetate (WanRosli et al. 2004).

The present study concerns the investigation of another form of cellulose derivative, namely cellulose phosphate, which has the potential as material for biomedical applications due to its biocompatibility and ability to induce the formation of apatite nuclei. For this purpose, microcrystalline cellulose (MCC) from EFB was chemically modified by phosphorylation and the obtained cellulose phosphate (EFB-CP) was characterized in terms of structural, surface morphology, crystallinity, and thermal stability. The biocompatibility of EFB-CP was assessed using mouse connective tissue fibroblast cells (L929) through the indirect extraction method, and its bioactivity was investigated by soaking the material for 30 days in a Simulated Body Fluid (SBF), where the ion concentration of the solution is approximately equal to human blood plasma.

## METHODOLOGY

### Synthesis of Oil Palm Empty Fruit Bunch (OPEFB) Cellulose Phosphate

Synthesis of OPEFB-CP was carried out by using the method described by WanRosli et al. (2010) based on the procedures of Granja et al. (2001). This method was

chosen because cellulose phosphate used as biomaterial must be free of any biologically hazardous compounds that might be present if using other alternative techniques (Vigo et al. 1974). Microcrystalline cellulose OPEFB (OPEFB-MCC) was obtained from OPEFB using the totally chlorine-free pulping and bleaching methods (WanRosli et al. 2003; Leh et al. 2008). To produce OPEFB-CP, OPEFB-MCC was first consecutively swollen in distilled water, ethanol, and hexanol for 24 hours each to activate the cellulose surface, followed by the phosphorylation reaction under an inert nitrogen atmosphere for 72 hours at 50 $^{o}$C. The final product was subsequently air-dried at room temperature and kept in desiccators over phosphorus pentoxide before characterization. The degree of substitution (DS) was calculated according to the procedure of Towle and Whistler (1972).

## Characterization of Cellulose Phosphate

Scanning electron microscopy (SEM) and energy dispersive analysis X-Ray (EDX) were carried out by using a SEM-EDX Oxford INCA 400 model at an acceleration voltage of 15kV. Fourier Transform Infrared (FTIR) spectroscopy was performed with a Perkin Elmer 1600 Infrared spectrometer using the KBr method. The samples were characterized for their thermal stability using a thermo gravimetric analyzer (TGA), model 2050 (TA Instruments, New Castle, DE); all specimens were scanned from 30$^{o}$C to 800$^{o}$C at the rate of 20$^{o}$C/min, and measurements were performed under a nitrogen flow. X-ray diffraction (XRD) was carried out by means of an X'Pert X-ray diffractometer (Siemens XRD D5000) using a Ni-filtered Cu Kα radiation at an angular incidence of 3° to 60° (2$\theta$ angle range). The operating voltage and current were 40 kV and 50 mA, respectively. The crystallinity of samples was calculated from diffraction intensity data using the empirical method as proposed by Segal et al. (1959) for native cellulose. The crystalline- to-amorphous ratio of materials was determined using the following equation,

$$CrI\ (\%) = [(I_{002} - I_{am}) / I_{002}] \times 100 \quad (1)$$

where $CrI$ is the crystallinity index, $I_{002}$ is the maximum intensity (in arbitrary units) of the diffraction from the (002) plane at 2 $\theta$ = 22.6°, and $I_{am}$ is the intensity of the background scatter measured at 2 $\theta$ =19.

## In Vitro Biocompatibility

*Material extraction*

The extraction process was carried out in accordance with ISO 10990-12 (1996). 2g of OPEFB-CP were sterilized for 4 hours under UV light, transferred into 50 mL centrifuge tubes, and then 10 mL of Dulbecco's Modified Eagle's Medium (DMEM) were added to the OPEFB-CP samples. The extraction was carried out for 72 hours at 37 °C in an incubator supplemented with $CO_2$, after which the materials were filtered using 0.2 μm syringe filters.

*Cell cultures*

L929 cell line from mouse skin fibroblasts (ATCC cell line CCL 1) were cultured in DMEM, which was supplemented with 10% fetal bovine serum (FBS) and 0.5%

antibiotics (penicillin/streptomycin). Cells were maintained at 37 °C in a humidified incubator with 5% $CO_2$ for 24 hours, until a monolayer, with greater than 80% confluence, was obtained. The cells were then detached by using 5 mL trypsin for cytotoxicity assay analysis (Serrano et al. 2005).

*Cytotoxicity evaluation (MTS assay)*

Cytotoxicity evaluation was performed using 96-well plates through the MTS assay, as described by Muzzarelli et al. (2005). 100 µL of L929 cells at a density of $1x10^4$ were placed in a 96-well plate, then incubated at 37°C for 24 hours in a 5% $CO_2$ environment. After 24 hours of incubation in DMEM supplemented with 10% fetal bovine serum (FBS) and 0.5% antibiotics (penicillin/streptomycin), the cells were treated by the indirect method with various concentrations of extracts of OPEFB-CP and incubated at 37 °C for another 72 hours in a 5% $CO_2$ environment. After 72 hours 20 µL aliquots of an MTS tetrazolium solution (MTS proliferation assay kit, Promega, Cell Titer 96 Aqueous One Solution Reagent) were added to the above cell cultures and incubated at 37 °C for 1 to 3 hours. Reduction of the MTS tetrazolium into a soluble formazan by viable cells was measured at OD 490 nm. The morphological changes of mouse skin fibroblast cells (L929) were observed by using an integrated microscope Zeiss-Axiovert 40-C.

Data values were expressed as means ± SD. Differences were compared by one-way analysis of variance (ANOVA) followed by Bonferroni correction. *P values* were considered to be statistically significant when $P < 0.05$.

*Cell proliferation assay*

Cells were seeded in 6-well plates at a density of $1x10^5$ cells/well and were incubated for 24 hours at 37 °C in an incubator supplemented with $CO_2$. After 24 hours, extracts at the $IC_{50}$ concentration identified by the MTS assay were added to the wells. Controls were exposed to culture medium supplemented with 10% fetal bovine serum (FBS) and 0.5% antibiotics (penicillin/streptomycin). After the treatment, cell incubation was extended for 8 days. Cell proliferation was evaluated using a trypan blue exclusion method (Altman et al. 1993). Cell counting was done by using Trypan Blue Solution 0.4% (Sigma). Briefly, cells were counted every day until the eighth day to identify the growth pattern of the treated and untreated cells. The cell growth medium and extracts were changed every 3 days. The cell proliferation graph was plotted up to 8 days. The morphological changes of mouse skin fibroblasts (L929) were observed by using an integrated microscope Zeiss-Axiovert 40-C.

*In vitro bioactivity assessment*

For the in vitro bioactivity study, 500 mg of OPEFB-CP were punched by using a rotary tablet machine model (LCY-RT-11) with 13 mm diameter and 3 mm width in size and treated in 20 mL $Ca(OH)_2$ solution for 24 hours at room temperature (Kawashita et al. 2003). Following this treatment, the samples were rinsed with distilled water and dried at room temperature. The samples were then soaked in 50 mL Simulated Body Fluid (SBF) inside a centrifuge tube for different periods of time. The SBF used has the following composition: 0.5 mM $Na_2SO_4$, 1.0 mM $K_2HPO_4{\cdot}3H_2O$, 4.2 mM $NaHCO_3$, 1.5

mM $MgCl_2 \cdot 6H_2O$, 2.5 mM $CaCl_2$, 136.8 mM NaCl, and 3.0 mM KCl; it was prepared in distilled water and was buffered at pH 7.25 with 50 mM TBS stabilized by HCl, and maintained at a constant temperature of 37 °C. After a given period, the specimens were washed with water and air-dried. The comparative amounts of ionic concentrations in mM of SBF and blood plasma as previously reported are listed in Table 1. The calcium phosphate formed on the surface of OPEFB-CP sample was characterized by FTIR, SEM-EDX, and XRD using monochromated Cu K$\alpha$ radiation with a step of $10^{o}$ $min^{-1}$ (Lin et al. 2009).

**Table 1.** Comparison of Ionic Concentration in mM of SBF and Blood Plasma

| | $Na^+$ | $K^+$ | $Mg^+$ | $Ca^{2+}$ | $Cl^-$ | $CO_3^{2-}$ | $HPO_4^{2-}$ |
|---|---|---|---|---|---|---|---|
| SBF | 142.0 | 5.0 | 1.5 | 2.5 | 143.8 | 4.2 | 1.0 |
| Blood Plasma | 142.0 | 5.0 | 1.5 | 2.5 | 103.0 | 27.0 | 1.0 |

source: Jalota et al. (2006)

## RESULTS AND DISCUSSION

### Characterization of Cellulose Phosphate (OPEFB-CP)

The phosphorylation of OPEFB-MCC was carried out using the $H_3PO_4/P_2O_5/Et_3PO_4$/hexanol method. Using the optimum conditions as reported by Wan Rosli et al. (2010), the produced OPEFB-CP had a degree of substitution (DS) of 2.4.

*Fourier Transforms Infrared Spectroscopy (FTIR)*

The FTIR spectra of unmodified and phosphorylated OPEFB-MCC are shown in Fig. 1. The major spectral peaks, as well as their corresponding peak assignments, are shown in Table 2.

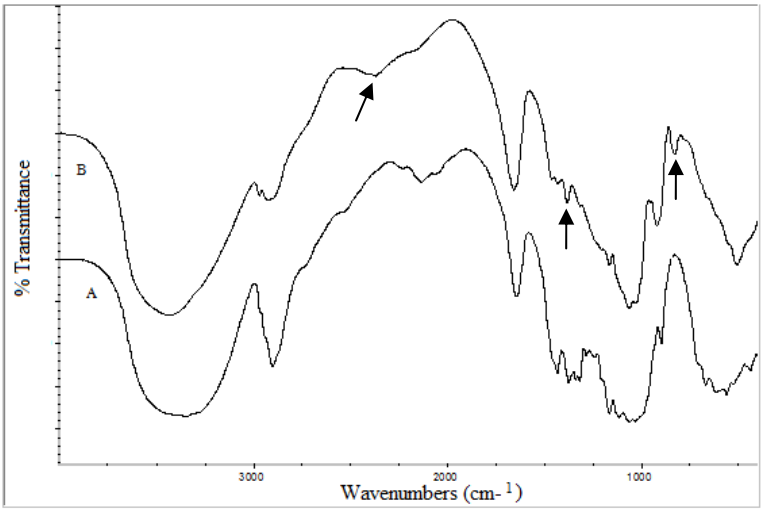


**Figure 1.** FTIR spectra of (A) microcrystalline cellulose (OPEFB-MCC) and (B) cellulose phosphate (OPEFB-CP)

The presence of new peaks (indicate by arrow) such as at 2380 $cm^{-1}$, corresponding to the P–H bond, 1380 $cm^{-1}$ corresponding to the P=O bonds, and a shoulder at 920 to 1000 $cm^{-1}$ attributable to the P–OH group, are indications of a successful phosphorylation reaction (Granja et al. 2001; Suflet et al. 2006).

**Table 2.** FTIR Spectral Peak Assignments of Unmodified and Phosphorylated OPEFB-MCC

| Peak frequency ($cm^{-1}$) | | Peak Assignment | References |
|---|---|---|---|
| Unmodified OPEFB-MCC | Phosphorylated OPEFB-MCC | | |
| 3400–3500 | 3400–3500 | OH groups | (WanRosli et al. 2011) |
| 2800–2900 | 2800–2900 | $CH_2$ groups | (Muller et al. 2006) |
| 1645 | 1647 | C=O stretching | (Granja and Barbosa 2001) |
| 1163 | 1168 | C–O–C stretching | (Granja et al. 2001) |
| - | 2380 | P–H stretching | (Suflet et al. 2006; WanRosli et al. 2011) |
| - | 1383 | P=O asymmetric stretching | (Jayakumar et al. 2009) |
| | 920–1000 | P–OH stretching | (Suflet et al. 2006; Granja et al. 2001) |
| | 825 | P–O–C stretching in phosphate ester | Suflet et al. 2006 |

## Scanning Electron Microscopy (SEM) and Energy Dispersive X-Ray (EDX) Analyses

Even though both unmodified and phosphorylated OPEFB-MCC showed a rough surface morphology, OPEFB-CP exhibited a more sponge-like surface character and compact structure (Figs. 2 (a) and (b)).

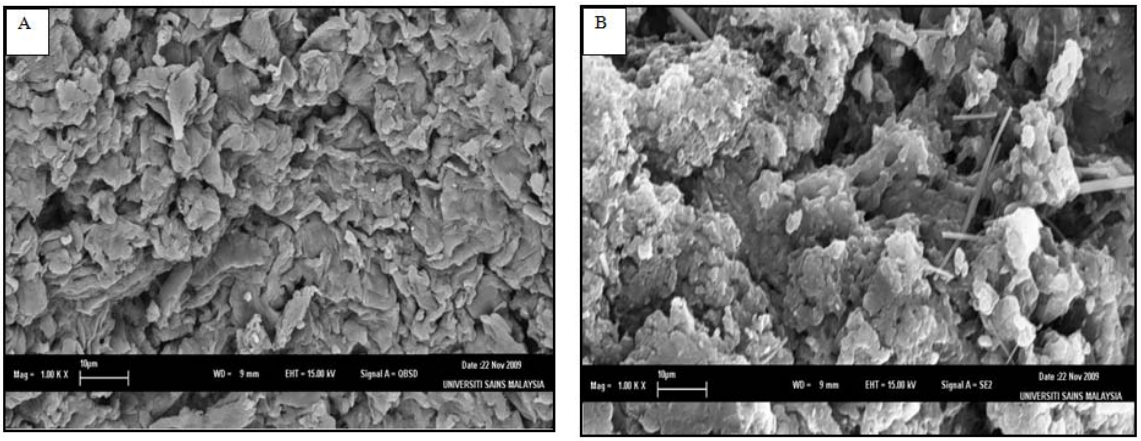


**Figure 2.** a) Unmodified OPEFB-MCC; and b) phosphorylated OPEFB-MCC

The elemental analysis (Table 3), as determined by energy dispersive x-ray (EDX) analysis, confirmed the presence of phosphorus with a 16.4% increase P upon phosphorylation. Concomitantly, there was also an 11.9% increase of O due to the substitution of OH groups by the phosphate groups containing additional O atoms (WanRosli et al. 2011).

**Table 3.** EDX Analysis of OPEFB-MCC and OPEFB-CP

| Element | OPEFB-MCC | OPEFB-CP | | |
|---|---|---|---|---|
| | Amount present, % | Amount present, % | Increase % | Decrease % |
| C | 55.79 | 34.16 | - | 38.77% |
| O | 44.21 | 49.45 | 11.85 | |
| P | - | 16.39 | 16.39 | - |
| Total | 100 | 100 | | |

## X-Ray Diffraction

X-ray diffraction (XRD) technique was used to determine the crystallinity index of both the unmodified OPEFB-MCC and its phosphorylated form. Remarkable changes were observed after phosphorylation, as Fig. 3 reveals. OPEFB-MCC exhibited a sharp diffraction peak between 19°-22.6° $\theta$, indicating that it has a crystalline structure with the diffractogram similar with that of wood MCC (Ardizzone et al. 1999). This suggests that they have the same polymorph, i.e., cellulose I. Calculated from the X-ray diffractograms using Eq. (1) (cf. Experimental section), the crystallinity of OPEFB-MCC was 87.9 %. After phosphorylation most of the diffraction bands were depressed or absent, demonstrating the loss of crystallinity. The introduction of phosphate groups onto the cellulose backbone disrupted the crystalline structure by virtue of decreasing the number of inter and intra-molecular hydrogen bonding, hence reducing the crystallinity of the original MCC cellulose (Gao et al. 2010; WanRosli et al. 2011). It was demonstrated that the derivation of cellulose diminishes the crystallinity of original samples (Suflet et al. 2006; Filho et al. 2007; Jayakumar et al. 2009).

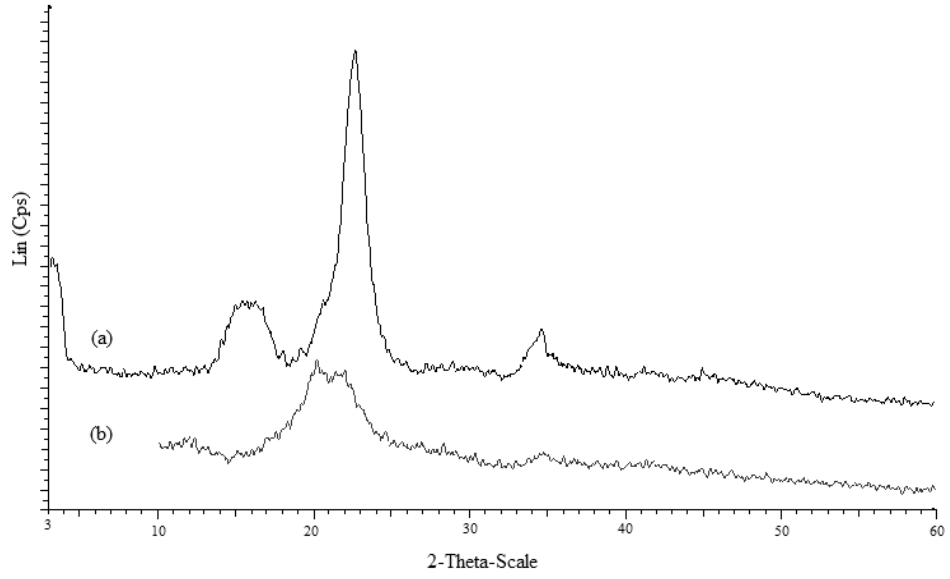


**Figure 3.** X- ray diffraction (XRD) patterns of (a) microcrystalline cellulose (OPEFB-MCC) and (b) cellulose phosphate (OPEFB-CP)

## Thermogravimetric Analysis

Thermal stability of OPEFB-MCC and OPEFB-CP was examined using thermogravimetric analysis (TGA) in the temperature range from 30 $^{o}$C to 900 $^{o}$C at a rate of 20 $^{o}$C/min under a nitrogen atmosphere. Figure 4 shows the TGA curves and its related derivative thermograms (DTG), whilst Table 3 presents the thermal behaviour of these materials using the on-set decomposition temperature ($T_{on}$) and temperatures at which various weight losses of the samples were recorded.

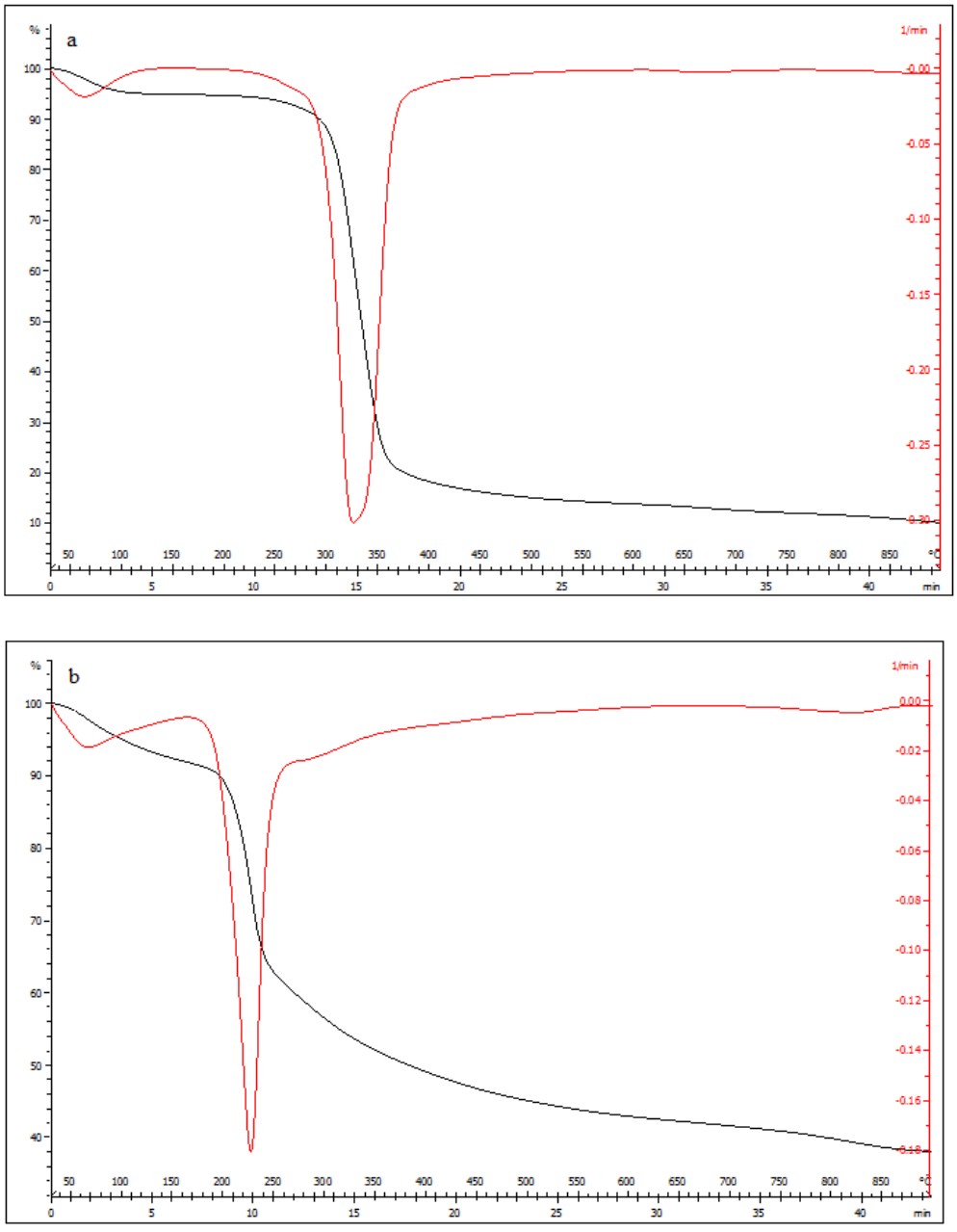


**Figure 4.** TGA and DTG curves of a) microcrystalline (OPEFB-MCC); and b) cellulose phosphate (OPEFB-CP) under $N_2$ atmosphere at 20 °C/min

As shown in Fig. 4, sample decomposition involves two main stages. In the first stage (temperature range between 30 °C and 180 °C) where the losses may be attributed to evaporation of moisture, it can be observed that OPEFB-MCC exhibited a weight loss of 6%, while for OPEFB-CP the weight loss was almost 9%. The higher weight loss for OPEFB-CP is a result of the increase in water content in the material following derivation (WanRosli et al. 2011; Barud et al. 2007; Suflet et al. 2006).

The second decomposition stage is believed to be due to pyrolysis and evolution of combustible gases. OPEFB-MCC and OPEFB-CP started to decompose at 254 °C and 180 °C respectively, the lower temperature of the latter indicating that the thermal stability of OPEFB-MCC is reduced upon phosphorylation, which has been explained in terms of reduced crystallinity (WanRosli et al. 2011; Barud et al. 2007). The greater thermal stability of OPEFB-MCC is also evidenced from DTG curves, where the decomposition peak temperature (denoted as $T_{1max}$) of OPEFB-MCC was at 327 $^{o}$C (Fig. 4a) and for OPEFB-CP (Fig. 4b) it was at 223$^{o}$C.

**Table 4.** Thermal Properties of OPEFB-MCC and OPEFB-CP

| Sample | Degradation Temperature (°C) | | | Residual Weight | DTG Peak Temperature ($^{o}$C). |
|---|---|---|---|---|---|
| | $T_{on}$ | $T_{10\%}$ | $T_{50\%}$ | % at 900 °C | $T_{1max}$ |
| OPEFB-MCC | 254 | 299 | 342 | 9.9 | 327 |
| OPEFB-CP | 180 | 196 | 376 | 37.9 | 223 |

It is however intriguing to note that at 50% weight loss (Table 4), the decomposition of OPEFB-CP occurred at a higher temperature than OPEFB-MCC (376 °C and 342 °C respectively). It can be conjectured that during the decomposition reaction some type of polymetaphosphoric acid is formed, which inhibits decomposition (Suflet et al. 2006). At 900 $^{o}$C (representing total decomposition), OPEFB-MCC presented a total loss of 90%, while the OPEFB-CP presented a loss of only 62%. The smaller rate of mass loss of OPEFB-CP may be due to some kind of thermal protection of the phosphate on the product, yielding more carbon than volatile products (Barud et al. 2007; Gao et al. 2010).

## In Vitro Biocompatibility

*Cytotoxicity (MTS assay)*

In consideration of the cellulose phosphate for potential use in biomedical devices, *in vitro* cytotoxicity tests were conducted on OPEFB-CP to evaluate its biocompatibility. This was assessed using L929 mouse fibroblast cells through the MTS assay. The extract dilution method (indirect method) involves a 72 hours incubation of OPEFB-CP extraction at 37 °C supplemented with $CO_2$, by exposure the cells to the extraction at different concentrations (mg/mL). This method was chosen over the direct exposure method to avoid confounding factors resulting from physical trauma to the cells (Melo et al. 2009).

Cytotoxicity tests, as revealed by Fig. 5a, showed that OPEFB-CP is non-cytotoxic. After 72 hours, the number of viable cells was observed to decrease with the increase in the concentration of extract added (mg/mL). At concentrations of 50 mg/mL to 25 mg/mL, values were significantly different from the control (at the levels of $p < 0.05$) and for the lower dilutions of 20 mg/mL to 3.125 mg/mL OPEFB-CP showed no significant differences from the control. At 50 mg/mL concentration, dilution of extraction inhibited the growth of L929 cells, for which the cell viability was less than 40%. The concentration for IC-50 (50% cell growth in culture medium) was 45 mg/mL and, at 35 mg/mL and lower, 70% of cells growing in culture survived. These observations are further confirmed by the percentage of dead cells (Fig. 5a), where there was a strong inverse correlation between concentration of dilution extraction and the percentage of dead cells. It can be seen that more than 90% of the cells died when the concentration of OPEFB-CP extraction was 50 mg/ml or greater, and less than 10% of the cells died when the concentration was less than 20 mg/mL. These phenomena can be explained in terms of acidity during the extraction, where most cellular functions, such as metabolism, cease at low pH (Wieslander et al. 1993). In our study, the pH of the culture medium was less than 4 at 50 mg/mL, and the value increased as the concentration of OPEFB-CP extraction was lowered.

Figures 5b-g show the cell morphology of L929 after 72 hours in culture medium at different concentrations. It is evident that the control culture of L929 cells was fairly transparent, with cells attached in a well confluent monolayer in medium (Fig. 5b), whereas with OPEFB-CP extraction, although a confluent monolayer was still observable up to a concentration of 45 mg/mL, cell density decreased with the increase in extract concentration.

(5a)

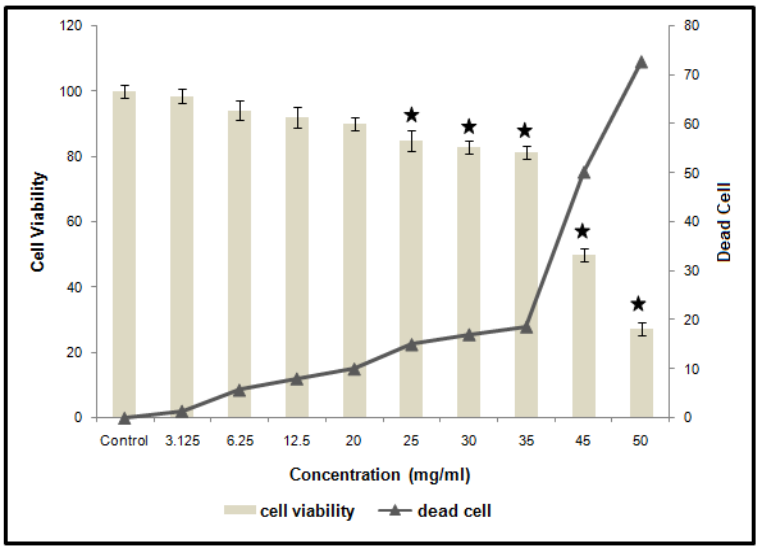


**Figure 5 (a).** Cytotoxicity assay of extracts (indirect method) of OPEFB-CP after 72 hours in culture with mouse skin fibroblast cells (L929). Mean ± SD (n = 3). (ANOVA) followed by Bonferroni correction indicated statistically significant difference when compared with the control (*$p \leq 0.05$); Cell morphology of L929 after 72hours in culture medium with different CP-EFB extraction concentrations.

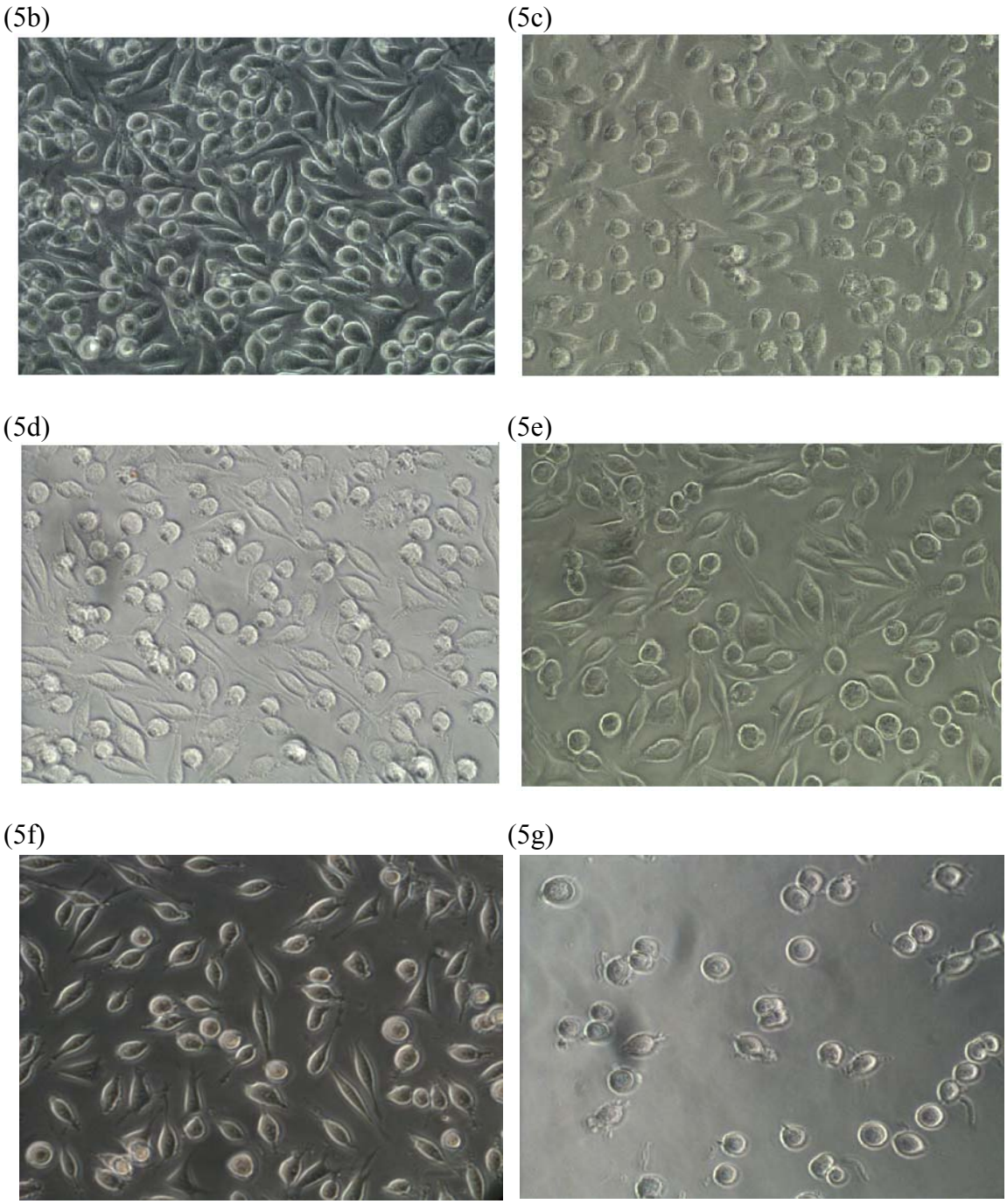


**Figure 5 (b through g).** Cytotoxicity assay of extracts (indirect method) of OPEFB-CP after 72 hours in culture with mouse skin fibroblast cells (L929). Mean ± SD (n = 3). (ANOVA) followed by Bonferroni correction indicated statistically significant difference when compared with the control (*p ≤ 0.05); Cell morphology of L929 after 72 hours in culture medium with different CP-EFB extraction concentrations: (5b) Control; (5c) 6mg/mL; (5d) 12.5mg/mL; (5e) 25mg/mL; (5f) 45mg/mL; and (5g) 50mg/mL OPEFB-CP (Magnification 40x).

*Cell proliferation*

The biocompatibility of OPEFB-CP was further evaluated in terms of its ability to promote cell proliferation. The proliferation assay of L929 cell line was carried out by allowing the cells to attach to a surface and grow with an IC-50 concentration extraction from OPEFB-CP, in comparison with cell culture in DMEM culture medium. Data are expressed as percentage of cell viability and cell concentration ($1x10^4$ cell/mL). Fig. 6a shows the percentage of viable L929 cells after 8 days in culture. The viability of the cells proliferated on the surfaces of these substrates generally increased with an increase in cell culturing time. The result showed no apparent inhibition effect of OPEFB-CP extraction on mouse skin fibroblast cells (L929) when an IC-50 concentration was used. The percentage of viable L929 cells increased from day 3 to day 8, where after 8 days in culture more than 70% of cell viability can be observed. As noted by Granja et al. (2006) phopshorylation promotes higher phosphate contents, which consequently yielded a more hydrophilic material. Such hydrophilicity can play a key role on cell growth and cell attachment, where it can promote higher or lower cell attachment and growth, depending on its value.

Fig. 6b shows the cell concentration of OPEFB-CP and control up to 8 days. The cell concentration of both sample increased with the increase in culture time. A similar trend was observed between OPEFB-CP extraction and the control (cells in medium); however OPEFB-CP showed a slower rate of proliferation where, after 8 days in culture, the concentrations of cells was $15x10^4$ cells/mL for OPEFB-CP treatment, and $20x10^4$ cells/mL for the control. Even though the cell growth in IC-50 concentration in the presence of OPEFB-CP was lower compared to control up to 8 days, the proliferation rate trend were similar, which indicates that OPEFB-CP at IC-50 concentration is biocompatible towards the L929 cell line. The microscopic analysis showed no changes in L929 cell morphology with IC-50 concentration treatment until 8 days in comparison to the control. The morphology cell of L929 cells appeared normal, similar to the control sample (Fig. 6c), which had large, spindle-shaped features, and the cells grew as a confluent monolayer.

*In vitro mineralization*

Mineralization of a material refers to the ability of materials to induce the formation of an apatite (calcium phosphate) layer when immersed in a simulated plasma solution (Barbosa et al. 2005; Muller et al. 2006; Kaputskii et al. 2007). In the present context it is often refereed as bioactivity. For this purpose, the calcium salt of cellulose phosphate was thus prepared by incubating OPEFB-CP with saturated $Ca(OH)_2$ aqueous solution for 24 hours. Mineralization tests followed by further soaking OPEFB-CP-Ca for 30 days in a simulated body fluid (SBF), where the ion concentrations are similar to human blood plasma.

Fig. 7 shows the FTIR spectrum of OPEFB-CP after immersion in SBF for various periods up to 30 days. Several new peaks were observed at 712.76 $cm^{-1}$, 819.91 $cm^{-1}$, 874 $cm^{-1}$, 1196.11 $cm^{-1}$, 1460.24 $cm^{-1}$, and 2504.96 $cm^{-1}$. According to Muller et al. (2006) vibration at 1460.24 $cm^{-1}$ can be assigned to the $Ca(OH)_2$ functionality, and peaks at 712.76 $cm^{-1}$ and 819.91 $cm^{-1}$ could be attributed to the stretching mode of carbonate $CO_3^{2-}$ ions.

(6a)

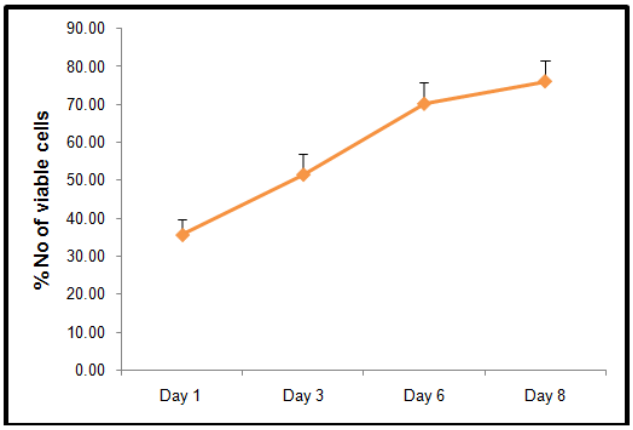


(6b)

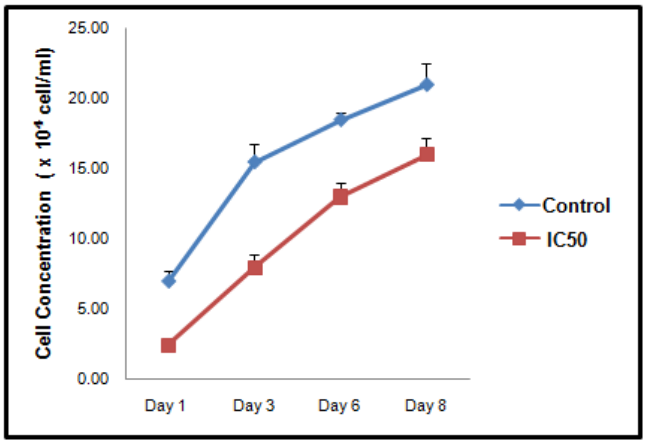


(6c) (6d)

**Figure 6.** a) Percentage of cell viability on cell proliferation, using L929 cells, up to 8 days with IC-50 concentration of OPEFB-CP; b) Cell concentration of L929 cells ($1x10^4$cell/mL) on cell proliferation up to 8 days with IC-50 concentration of OPEFB-CP compared to control (cells in DMEM); c) L929 Cell morphology after eight days in culture, treated with OPEFB-CP at IC-50 concentration; and d) L929 cells morphology after eight days in Dulbecco Modified Eagle Medium (DMEM) (Magnification 20x).

Such ions form due to the reaction of $Ca(OH)_2$ with $CO_2$ dissolved in water at atmospheric pressure during the treatment of OPEFB-CP in $Ca(OH)_2$ solution (Li et al. 1997b; Muller et al. 2006). The sharp peak at 874 $cm^{-1}$ is indicative of deposition of an apatite layer on the surface of OPEFB-CP after 3 days of immersion in SBF. As the apatite layer grew on the surface of OPEFB-CP, the peaks at 874 $cm^{-1}$ became sharp and dominant in the FTIR spectra (Lin et al. 2009). The broad band at 1072.88 $cm^{-1}$ for OPEFB-CP can be identified as apparently carbonate containing calcium phosphate based on carbonate ion bands appearing in FT-IR spectra (Ban and Maruno 1998; Ekholm et al. 2005).

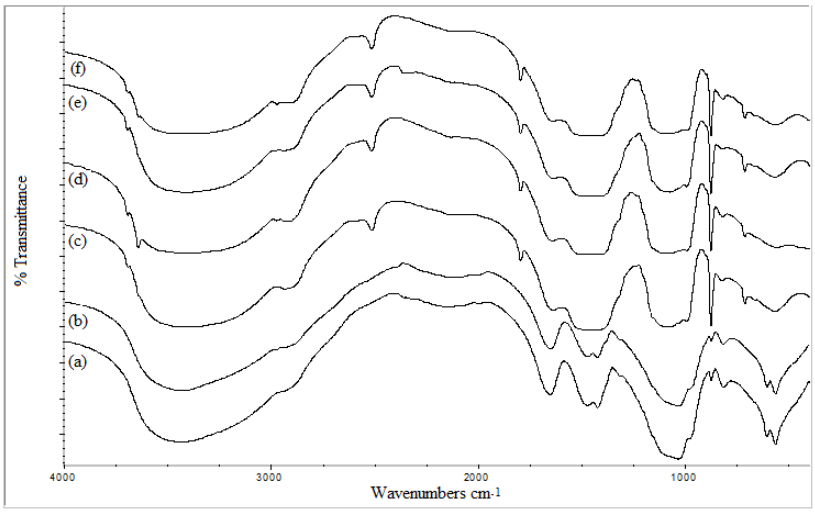


**Figure 7.** FT-IR analysis OPEFB-CP-Ca after incubation in simulated body fluid (SBF) for 30 days. (a) 0 days; (b) 1 day; (c) 3 days; (d) 6 days; (e) 15 days; (f) 30 days

The detection of the presence of $PO_4^{3-}$ groups in the sample surface was carried out using SEM-EDX and XRD in order to further understand apatite formation on OPEFB-CP.

SEM observations (Fig. 8) showed the formation of an apatite layer on the surfaces of OPEFB-CP after incubation in SBF for 30 days. Some mineral deposits, which are attributable to apatite nuclei, could be observed on the surface of OPEFB-CP after 3 days in SBF. According to Kawashita et al. (2003), after being treated with the saturated $Ca(OH)_2$ solution, a large number of the calcium ions remains attached to the surface of the material, while during the subsequent soaking in the SBF, some of these calcium ions are released into the SBF. As a result, the ionic activity product of the apatite in the surrounding SBF increases and accelerates apatite nucleation; and once the apatite nuclei are formed, they spontaneously grow by consuming the calcium and phosphate ions from the surrounding fluid. Therefore, by increasing the soaking time, apatite formation was clearly shown after 3 days in SBF up to 15 days. According to Martins et al. (2009), immersion in SBF solution for over a period promotes the growth of apatite nuclei layer, which help in forming a dense and compact apatite nuclei on the surface of a material. The apatite formation is shown in Fig. 8 (Figs. b through g). Frame (h) shows the detailed morphology of the apatite layer formed after 30 days in SBF (at 10000x magnification).

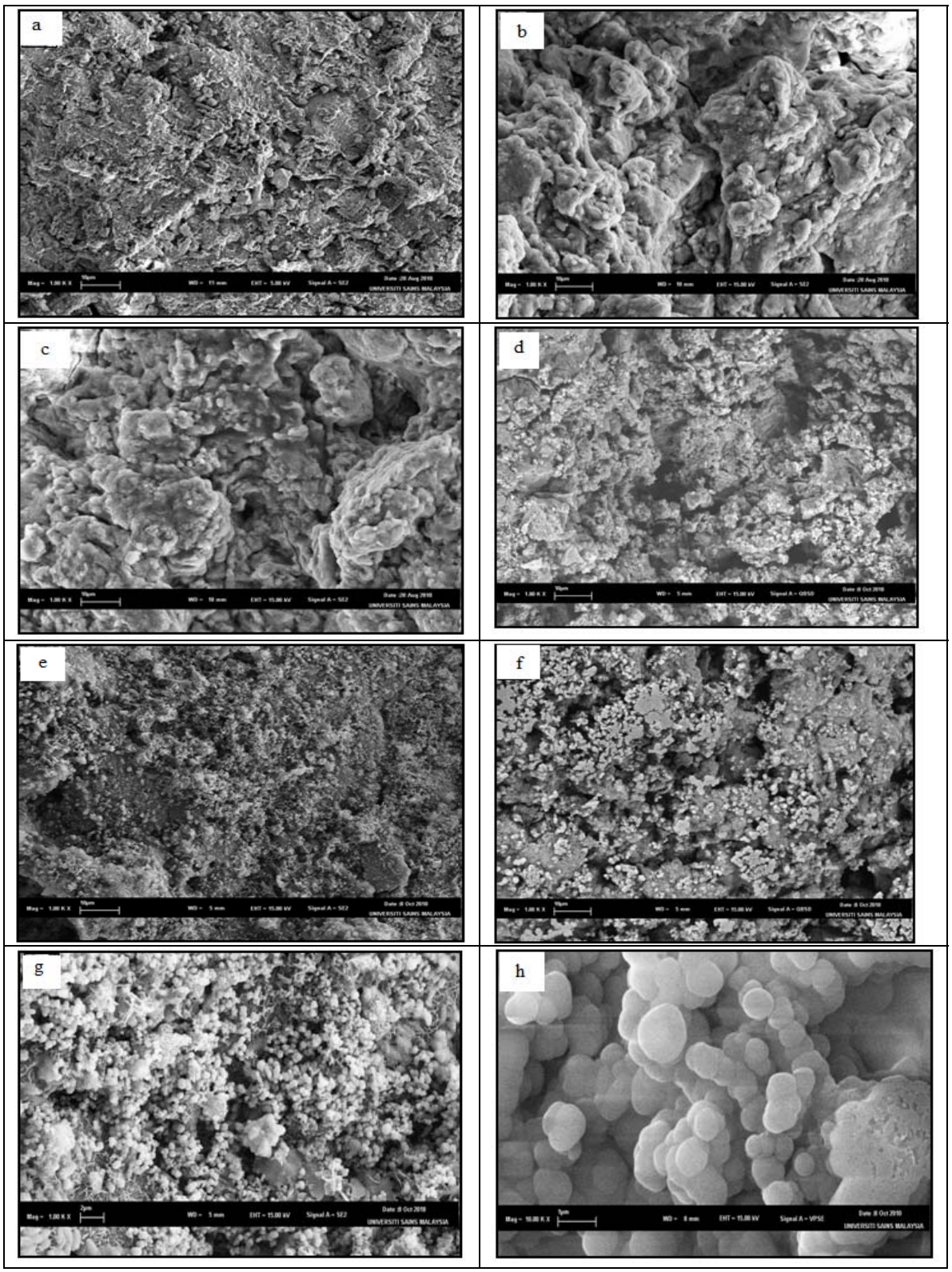


**Figure 8.** SEM photomicrographs of OPEFB-CP surfaces treated with $Ca(OH)_2$ before and after soaking in the SBF for various periods: (a) 0 days; (b) 1day; (c) 3 days; (d) 6 days; (e)15 days; (f) 24 days and (g) 30 days; (h) 10000x magnification of (g). (a-g magnification 1000x)

EDX analysis was performed in order to determine the molar ratio between calcium (Ca) and phosphorus (P) after soaking OPEFB-CP in SBF for up to 30 days. EDX analysis revealed that calcium, phosphorus, and oxygen accumulated on the surface of OPEFB-CP soaking in SBF, which can be identified as a calcium a phosphate layer (Li et al.1997a).

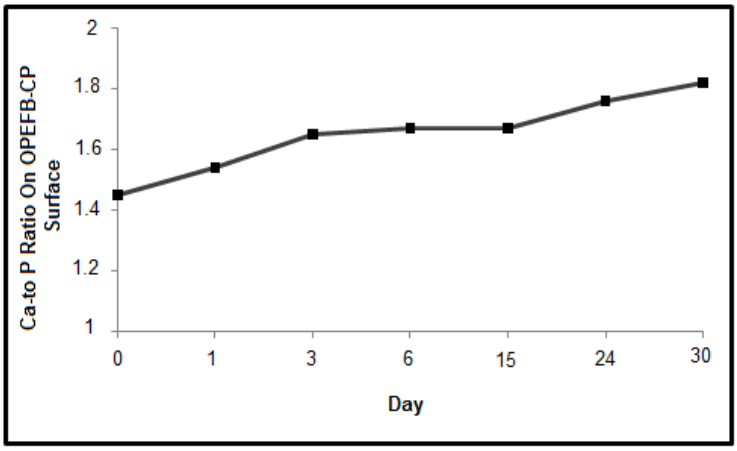


**Figure 9.** Changing trend of Ca to P ratio on the surface of OPEFB-CP samples after immersed in SBF, as detected by SEM-EDX

The Ca/P ratio of OPEFB-CP ranged from 1.54 to 1.84 (Fig. 9) after 30 days of immersion in SBF. Higher Ca:P ratios suggest Ca-enrichment due to the treatment OPEFB-CP with $Ca(OH)_2$. It is assumed that $Ca(OH)_2$ partially hydrolyzed the OPEFB-CP $PO_4$ groups to produce perhaps OCP at an initial phase, which is then rapidly transformed into apatite. It has been speculated that octacalcium phosphate (OCP) is the preferred precursor for super-saturation in solutions containing $Ca^{2+}$ and $PO_4$ ions (Yokogawa et al. 1997).

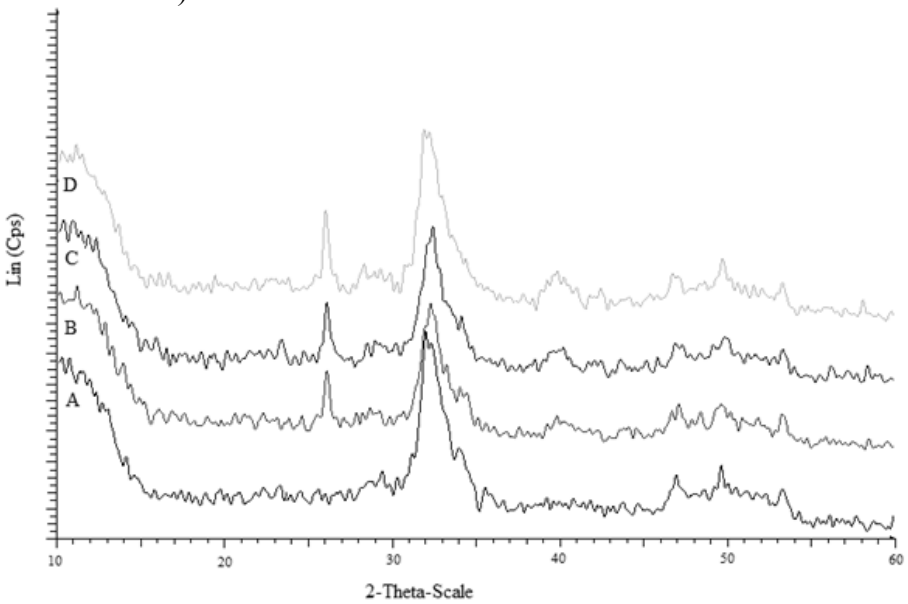


**Figure 10.** XRD patterns of the OPEFB-CP before and after immersed in SBF for (a) 0 days; (b) 3 days; (c) 15 days; and (d) 30 days

The XRD patterns of OPEFB-CP surfaces immersed in the SBF, as shown in Fig. 10, provide evidence that the calcium phosphate apatite was formed on the surface of OPEFB-CP. After 3 days in SBF and up to 30 days, the characteristic peak of apatite at $2\theta$ = 26.10° appeared after immersion in simulated body fluid (SBF) (Lin et al. 2009; Hayashi et al. 2009). The sharp peak at 2 $\theta$ =32.10° in all samples can be attributed to $Ca(OH)_2$, according to matching with International Centre diffraction data (ICDD). After 3 days in SBF a $CaCO_3$ phase appeared, revealed by peaks at $2\theta$ = 37.86° and 58.86°, which was attributed to carbonization of $Ca(OH)_2$ by incorporating $CO_3^{-2}$ from SBF (Lin et al. 2009).

## CONCLUSIONS

1. Cellulose phosphate gel was successfully synthesized from OPEFB-MCC using the $H_3PO_4/P_2O_5/Et_3PO_4$/hexanol method.
2. Changes in surface morphology of OPEFB-CP, disruption of crystalline structure of OPEFB-MCC, the presence of new FTIR peaks on OPEFB-CP at 2380 $cm^{-1}$ and 1380 $cm^{-1}$, a shoulder at 920 to 1000 $cm^{-1}$, and a smaller rate of mass loss of OPEFB-CP due to some kind of thermal protection of the phosphate are indications of a successful phosphorylation reaction.
3. OPEFB-CP showed non-cytotoxic behaviour in *in vitro* biocompatibility studies, depending on the concentration used, where the IC-50 value was 45 mg/mL; however above this IC-50 concentration limit, the material can be considered toxic to the L929 cell line.
4. OPEFB-CP showed good proliferation rate of up to 8 days when the IC-50 concentration was used, and no morphological changes was observed below that IC-50 concentration.
5. OPEFB-CP showed good mineralization capability by inducing the formation of an apatite layer after 30 days in SBF, as confirmed by SEM/EDX with Ca to P molar ratio up to 1.84. The characteristic peak of apatite at $2\theta$ = 26.10° appeared after 3 days immersion in SBF, and an FTIR peak at 874 $cm^{-1}$ indicated the deposition of an apatite layer on the surface of OPEFB-CP.

## ACKNOWLEDGEMENTS

The authors would like to thank Universiti Sains Malaysia for its financial support under research grant 1001/PTEKIND 8141051, Ministry of Higher Education Malaysia (KPT) for sponsoring postgraduate studies of M.K Mohamad Haafiz, and Craniofacial Lab Staff member Eda Binti Sarip PPSG USMKK for her help and discussion.

## REFERENCES CITED

Alriols, M. G., Tejado, A., Blanco, M., Mondragon, I., and Labidi, J. (2009). "Agricultural palm oil tree residues as raw material for cellulose, lignin and

hemicelluloses production by ethylene glycol pulping process," *Chemical Engineering Journal* 148, 106-114.

Altman, S. A., Randers, L., and Rao. G. (1999). "Comparison of trypan blue dye exclusion and fluorometric assays for mammalian cell viability determinations," *Biotechnol. Rag*. 9, 871-874.

Ardizzone, S., Dioguardi, F. S., Mussini, T., Mussini, P. R., Rondinini, S., Vercelli, B., and Vertova, A.(1999). "Microcrystalline cellulose powders: Structure, surface features and water sorption capability," *Cellulose* 6, 57-69.

Ban, S., and Maruno, S. (1998). "Morphology and microstructure of electrochemically deposited calcium phosphates in a modified simulated body fluid," *Biomaterials* 19, 1245-1253.

Barbosa, M. A., Granja, P. L., Barrias, C. C., and Amaral, I. F. (2005). "Polysaccharides as scaffolds for bone regeneration," *ITBM-RB*. 26, 212-217.

Barud, H. S., Ribeiro, C. A., Crespi, M. S., Martines, M. A. U., Dexpert-Ghys, J., Marques, R. F. C., Messaddeq, Y., and Ribeiro, S. J. L. (2007). "Thermal characterization of bacterial cellulose-phosphate composite membranes," *Journal of Thermal Analysis and Calorimetry* 87 (3), 815-818.

Burg, K. J. L., Porter, S., and Kellam, J. F. (2000). "Biomaterial developments for bone tissue engineering," *Biomaterials* 21, 2347-2359.

Correlo, V. M., Boesel, L. F., Pinho, E., Costa-Pinto, A. R., Alves da Silva, M. L. Bhattacharya, M., Mano, J. F., Neves, N. M., and Reis, R. L. (2008). "Melt-based compression-molded scaffolds from chitosan–polyester blends and composites: Morphology and mechanical properties," *J. Biomed Mater Res. Part A* 489-504.

Ekholm, E., Tommila, M., Forsback, A. P., Martson, M., Holmbom, J., Finnberg, C., Kuusilehto, A., Salonen, J., Yli-Urpo, A., and Penttinen, R. (2005). "Hydroxyapatite coating of cellulose sponge does not improve its osteogenic potency in rat bone," *Acta Biomaterialia* 1, 535-544.

Entcheva, E., Bien, H., Yin, L., Chung, C.Y., Farrell, M., and Kostov, Y. (2004). "Functional cardiac cell constructs on cellulose-based scaffolding," *Biomaterials* 25, 5753-5762.

Filho, G. R., Assuncao, R. M. N., Vieira, J .G., Meireles, C. S., Cerqueira, D. A., Barud, H. S., Ribeiro, S. J. L., and Messaddeq, Y. (2007). "Characterization of methylcellulose produced from sugar cane bagasse cellulose: Crystallinity and thermal properties," *Polymer Degradation and Stability* 92, 205-210.

Fricain, J. C., Granja, P. L., Barbosa, M. A., Jeso, B. D., Barthe, N., and Baquey, C. (2002). "Cellulose phosphates as biomaterials. In vivo biocompatibility studies," *Biomaterials* 23, 971-980.

Gao, C., Xiong, G. Y., Luo, H. L., Ren, K. J., Huang, Y., and Wan, Y. Z. (2010). "Dynamic interaction between the growing Ca–P minerals and bacterial cellulose nanofibers during early biomineralization process," *Cellulose*17, 365-373.

Granja, P. L., and Barbosa, M. A. (2001). "Cellulose phosphate as biomaterials. Mineralization of chemically modified regenerated cellulose hydrogels," *J. Materials Science* 36, 2163-2172.

Granja, P. L., De Jéso, B., Bareille, R. Rouais, F., Baquey C., and Barbosa, M. A. (2005). "Mineralization of regenerated cellulose hydrogels induced by human bone marrow stromal cells," *European Cell and Materials* 10, 31-39.

Granja, P. L., De Jéso, B., Bareille, R., Rouais, F., Baquey C., and Barbosa, M. A. (2006). "Cellulose phosphates as biomaterials. In vitro biocompatibility studies," *Reactive & Functional Polymers* 66, 728-739.

Granja, P. L., Pouyse'gu, L., Deffieux, D., Daude, G., and Barbosa, M. A. (2001). "Cellulose phosphates as biomaterials. II. Surface chemical modification of regenerated cellulose hydrogels," *J. Appl. Poly. Sci.* 82, 3354-3365.

Hayashi, S., Ohkawa, K., Yamamoto, H., Yamaguchi, M., Kimoto, S., Kurata, S., and Shinji, H. (2009). "Calcium phosphate crystallization on electrospun cellulose non-woven fabrics containing synthetic phosphorylated polypeptides," *Macromol. Mater. Eng.* 294, 315-322.

International Standard Office (1996). "Biological evaluation of medical devices. Part 12: Sample preparation and reference material," ISO 10993-12, Geneva 20, Switzerland.

Jalota, S., Bhaduri, S. B., and Tas. A. C. (2006). "Effect of carbonate content and buffer type on calciumphosphate formation in SBF solutions," *J. Mater Sci: Mater Med.* 17, 697-707.

Jayakumar, R., Egawa, T., Furuike, T., Nair, S. V., and Tamura, H. (2009). "Synthesis, characterization, and thermal properties of phosphorylated chitin for biomedical applications," *Polym. Eng. Sci.* 49, 844-849.

Kaputskii, F. N., Yurkshtovich, N. K., Yurkshtovich, T. L., Golub, N. V., and Kosterova, R. I. (2007). "Preparation and physicochemical and mechanical properties of low-substituted cellulose phosphate fibers," *Russian J. Appl. Chem*. 80, 1135-1139.

Kawashita, M., Nakao, M., Minoda, M., Kima, H.M., Beppu, T., Miyamoto, T., Kokubo, T., and Nakamura, T. (2003). "Apatite-forming ability of carboxyl group-containing polymer gels in a simulated body fluid," *Biomaterials* 24, 2477-2484.

Leh, C. P., Wan Rosli, W. D., Zainuddin, Z., and Tanaka, R. (2008). "Optimisation of oxygen delignification in production of totally chlorine-free cellulose pulps from oil palm empty fruit bunch fibre," *Industrial Crops and Products* 28, 260-267.

Li, S. H., Liu, Q., de Wijn, J., Wolke J., Zhou, B., and de Groot, K. (1997b). "In-vitro apatite formation on phosphorylated bamboo," *Journal of Materials Science*: *Materials in Medicine* 8, 543-549.

Li, S. H., Liu, Q., de Wijn, J., Zhou, B. L., and De Groot, K. (1997a). "In vitro calcium phosphate formation on a natural composite material, bamboo," *Biomoterials* 18, 389-395.

Lin, Q., Li, Y., Lan, X. Lu, C., Chen, Y., and Xu. Z. (2009). "The apatite formation ability of $CaF_2$ doping tricalcium silicates in simulated body fluid," *Biomed. Mater*. DOI 10.1088/1748-6041/4/4/045005.

Martins, A. M., Pereira, R. C., Leonor, I. B., Azevedo, H. S., and Reis, R. L. (2009). "Chitosan scaffolds incorporating lysozyme into CaP coatings produced by a biomimetic route: A novel concept for tissue engineering combining a self-regulated degradation system with in situ pore formation," *Acta Biomaterialia* 5, 3328-3336.

Matthew, H. W. T. (2002). "Polymers for tissue engineering scaffolds," In: *Polymeric Biomaterial Polymeric Biomaterial*, 2nd Ed., Marcel Dekker, Inc. (Chapter 8).

Melo, A. D., Bet, A. C., Assreuy, J., Debacher, N. A., and Soldi, V. (2009). "Adhesion of L929 mouse fibroblast cells on poly(styrene)/poly(methyl methacrylate) films," *J. Braz. Chem. Soc.* 20,1753-1757.

Muller, F. A., Muller, L., Hofmann, I., Greil, P., Wenzel, M. M., and Staudenmaier, R. (2006). "Cellulose-based scaffold materials for cartilage tissue engineering," *Biomaterials* 27, 3955-3963.

Muzzarellia, R. A. A., Guerrierib, M., Goteric, G., Muzzarellia, C., Armenid, T., Ghisellie, R., and Cornelissenf, M. (2005). "The biocompatibility of dibutyryl chitin in the context of wound dressings," *Biomaterials* 26, 5844-5854.

Nair, L. S., and Laurencin, C. T. (2005). "Polymers as biomaterials for tissue engineering and controlled drug delivery," *Adv Biochem Engin/Biotechnol.* 102, 47-90.

Nair, L. S., and Laurencin, C. T. (2007). "Biodegradable polymers as biomaterials," *Prog. Polym. Sci*. 32, 762-798.

Segal, L., Creely, J. J., Martin, Jr., A. E., and Conrad, C. M. (1959). "An empirical method for estimating the degree of crystallinity of native cellulose using the X-ray diffractometer," *Textile Research Journal* 29,786-794.

Serrano, M. C., Pagani, R., Pena, J., and Portoles, M. T. (2005). "Transitory oxidative stress in L929 fibroblasts cultured on poly (ε-caprolactone) films," *Biomaterials* 26, 5827-5834.

Suflet, D. M., Chitanu, G. C., and Popa, V. I. (2006). "Phosphorylation of polysaccharides: New results on synthesis and characterisation of phosphorylated cellulose," *Reactive & Functional Polymers* 66, 1240-1249.

Towle, G. A., and Whistler, R. L. (1972). "Phosphorylation of starch and cellulose with an amine salt of tetrapolyphosphoric acid," In: R. L. Whistler (Ed.). *Methods of Carbohydrate Chemistry*, Academic Press, New York, 6, 408-411.

Vepari, C., and Kaplan, D. L. (2007). "Silk as a biomaterial," *Prog. Polym. Sci.* 32, 991-1007.

Vigo, T. L., and Welch, C. M. (1974). "Chlorination and phosphorylation of cotton cellulose by reaction with phosphoryl chloride in *N,N*-dimethylformamide," *Carbohydrate Research* 32, 331-338.

Wan Rosli, W. D., Law, K. N., and Valade, J. L. (1998). "Chemical pulping of oil palm fruit bunches," *Cell. Chem. Technol.*32, 133-143.

Wan Rosli, W. D., Leh, C. P., Zainuddin, Z., and Tanaka, R. (2003). "Optimization of soda pulping variable for preparation of dissolving pulps from oil palm fiber," *Holzforschung* 57, 106-113.

Wan Rosli, W. D., Leh, C. P., Zainuddin, Z., and Tanaka. R. (2004). "The effects of prehydrolysis on the production of dissolving pulp from empty fruit bunches," *J. Tropical Forest Science* 16(3), 343-349.

Wan Rosli, W. D., Zainuddin, Z., Law, K.N., and Asro, R. (2007). "Pulp from oil palm fronds by chemical processes," *Industrial Crops and Products* 25, 89-94.

Wan Rosli, W. D., Rohaizu, R., and Ghazali, A. (2011). "Synthesis and characterization of cellulose phosphate from oil palm empty fruit bunches," *Carbohydrate Polymers* 84, 262-267.

Wieslander, A. P., Andren, A., and Martinson, E. (1993). "Toxicity of effluent peritoneal dialysis fluid," *Bio Info Bank Library* 31-35.

Yokogawa , Y., Paz Reyes, J., Mucalo, M. R., Toriyama, M., Kawamoto, Y., Suzuki, T., Nishizawa, K., Nagata, F., and Kamayama, T. (1997). "Growth of calcium phosphate on phosphorylated chitin fibres," *Journal of Materials Science: Materials in Medicine* 8, 407-412.

Article submitted: December 26, 2011; Peer review completed: February 13, 2011; Revised version received and accepted: March 28, 2011; Published: March 29, 2011.